ChemElectroChem

Supporting Information

Strong Activity Changes Observable during the First Pretreatment Cycles of Trimetallic PtNiMo/C Catalysts

Bilal Danisman, Gui-Rong Zhang, Adrian F. Baumunk, Juntao Yang, Olaf Brummel, Philipp Darge, Karl J. J. Mayrhofer, Jörg Libuda, Marc Ledendecker, and Bastian J. M. Etzold*

Additional references cited within the Supporting Information.[23],[29],[35],[48]

Table of contents

Synthesis of PtNiMo/C catalyst:

The synthesis of carbon supported PtNiMo catalyst was carried out by using a surfactant free solvothermal method following literature procedures.[29],[35] A typical protocol is as follows: $Pt(acac)_2$ (94.5 mg, 0.24 mmol), $Ni(acac)_2$ (55.6 mg, 0.22 mmol), $Mo(CO)_6$ (2.2 mg, 0.007 mmol) and Benzoic acid (586,2 mg, 4.80 mmol) were dissolved in 12 mL of DMF by 10 minutes of ultrasonication. The solution was transferred into a 23 mL Teflon lined stainless steel autoclave from Parr Instrument and after adding Ketjenblack EC-300J (126.4 mg) it was sealed and put into a preheated oven at 200 °C. After 24 h of synthesis, the autoclave was removed from the oven and allowed to cool down to room temperature in the fume hood naturally. The resulting nanoparticles on Ketjenblack were treated ultrasonically for 30 min and dispersed in ethanol afterwards, which was stirred for 3 days. The washing procedure was performed within three wash cycles, which consisting of centrifugation, decanting the supernatant, adding fresh solvent and dispersing the mixture by ultrasonic treatment, respectively. As solvent ethanol (ultrapure, denatured) was used for the first two cycles and acetone (ultrapure) was used for the third cycle continued by filtered the mixture and once more cleaned with acetone, water (ultrapure) and ethanol (absolute) until filtrate was colorless. The received catalyst was dried overnight at 80 °C under vacuum.

Structural characterization

ICP-OES analysis to determine the sample compositions was conducted and obtained a Pt-loading of 22.2 wt. % and a final atomic composition of Pt:Ni:Mo = 1:0.61:0.0035. The STEM analysis (**Figure S1a-b)** reveals a uniformly distribution of octahedral shaped nanoparticles over the carbon support with a low content of aggregation. An additional insight into the characterization of the catalyst is also shown in our work[23] on a similar catalyst. The TEM images show a uniform distribution of the octahedral shaped PtNiMo nanoparticles on the carbon surface with an overall particle size of 6.0 (+0.9) nm. Further, this catalyst provides a Pt-loading of 17.3 wt. % and an atomic composition of Pt:Ni:Mo = 1:0.44:0.01, confirming the success of the synthesis procedure. From the XRD analysis (**Figure S1c**) we can see a similar behavior of all diffraction peaks shown in our previous work[23]. Herein, also a shift toward higher angles in compare to the reference Pt results, which indicates Pt lattice contraction due to alloying Pt with transition metals (Ni, Mo). Further, no additional peak from Ni or Mo species can be detected in the XRD pattern, which confirms the formation of a single Pt-based alloy phase.

Electrochemical Measurements:

In addition to the electrochemical measurements, the IR-drop effect was compensated for all ORR measurements. Herein, the ohmic resistance was determined by conducting electrochemical impedance spectroscopy (EIS) analysis with an AC signal analysis (5 mV, 10 kHz). The mass-transport corrected kinetic current (i_k) which used for evaluating the ORR performance was calculated based on the *Koutecký-Levich* equation:[42]

$$\frac{1}{i} = \frac{1}{i_k} + \frac{1}{i_d} \qquad \text{(S1)}$$

Where i is the experimentally measured current from the positive going polarization curves, which is background current corrected (in N_2-saturated electrolyte), i_d is the diffusion limiting current and i_k the kinetic current. Obtained kinetic currents were normalized to the ECSA or mass of Pt to obtain the specific activity (SA) or mass-specific activity (MSA) of Pt, respectively.

Supplementary figures:

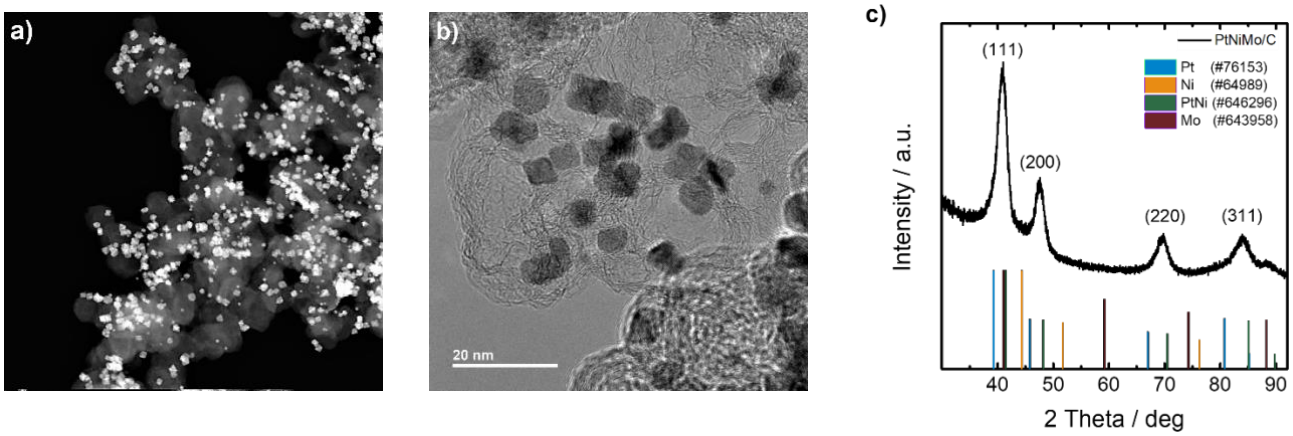

Figure S1: a-b) STEM image of PtNiMo nanoparticles supported on Ketjenblack EC-300J. b) XRD diffraction peaks with assigned peaks from Inorganic Crystal Structure Database (ICSD).

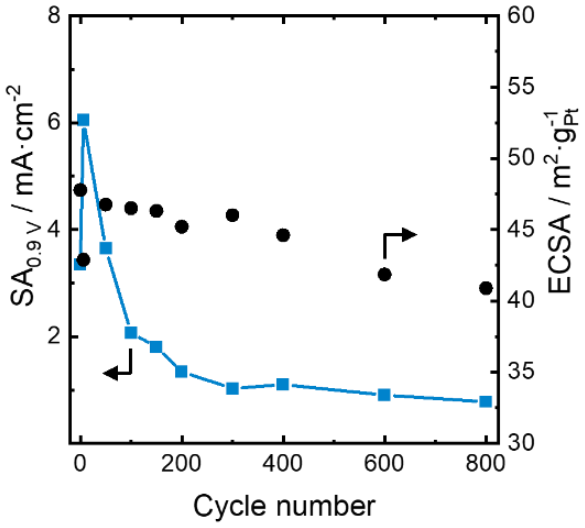

Figure S2: Specific activities at 0.90 V_{RHE} in O_2 and ECSA development throughout increasing conditioning cycle numbers from initial to 800 cycles for PtNiMo/C. Potential range: 0.05-1.20 V_{RHE}, ORR at 20 mV s^{-1} with rotation at 1600 rpm in saturated 0.1 M $HClO_4$ solution.

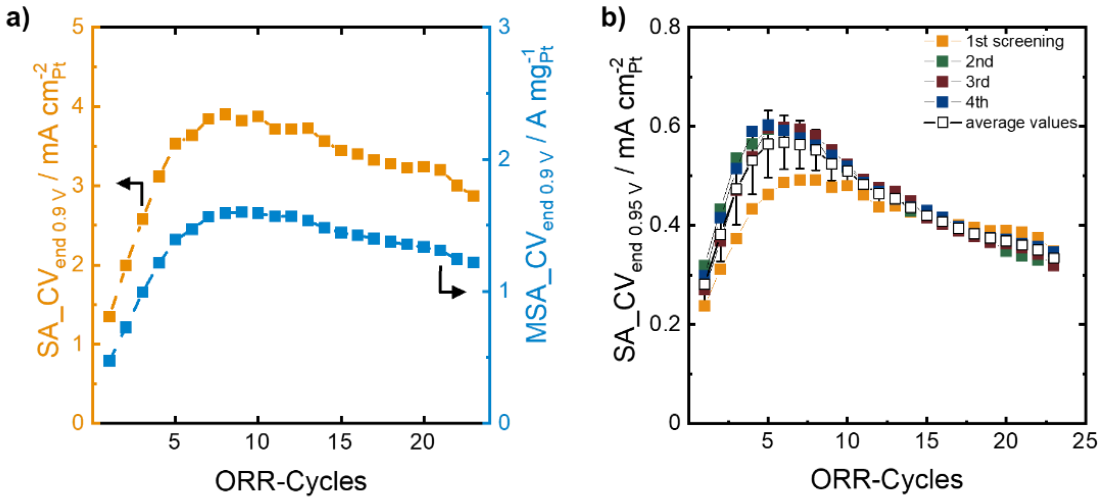

Figure S3: a) SA_CV_{end} and MSA_CV_{end} progress in dependence of ORR cycle numbers at 0.90 V_{RHE}. b) Average SA_CV_{end} screening values (unfilled squares) and repeating measurements (filled squares) at 0.95 V_{RHE} from different catalyst inks of PtNiMo/C. Recorded in O_2-saturated 0.1 M $HClO_4$ electrolyte (potential range: 0.05-1.20 V_{RHE}; scan-rate: 20 mV s^{-1} with rotation at 1600 rpm).

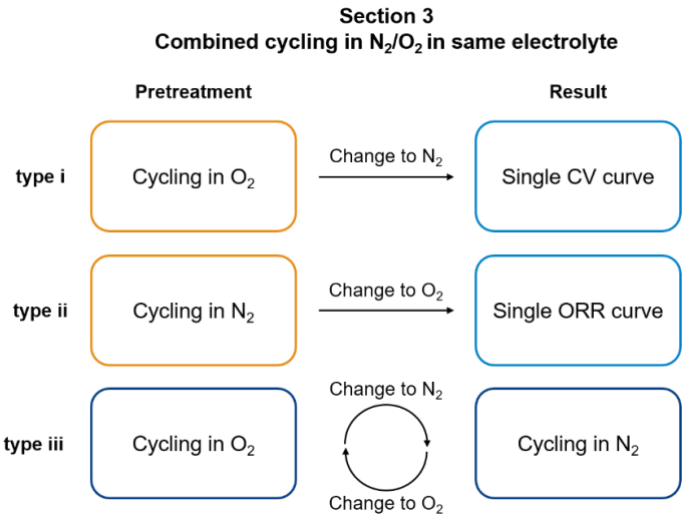

Scheme S1: Experimental protocol scheme for PtNiMo/C in section 3. Shown are the pretreatment cycles in N_2 or O_2, the change of atmosphere and resulting curves as CV or polarization curve for ORR in the same electrolyte. In type iii), several numbers of cycles are done in repeating change of atmosphere in the same electrolyte. Potential range: 0.05-1.20 V_{RHE} at 20 mV s^{-1}, ORR with rotation at 1600 rpm in O_2 saturated 0.1 M $HClO_4$ solution.

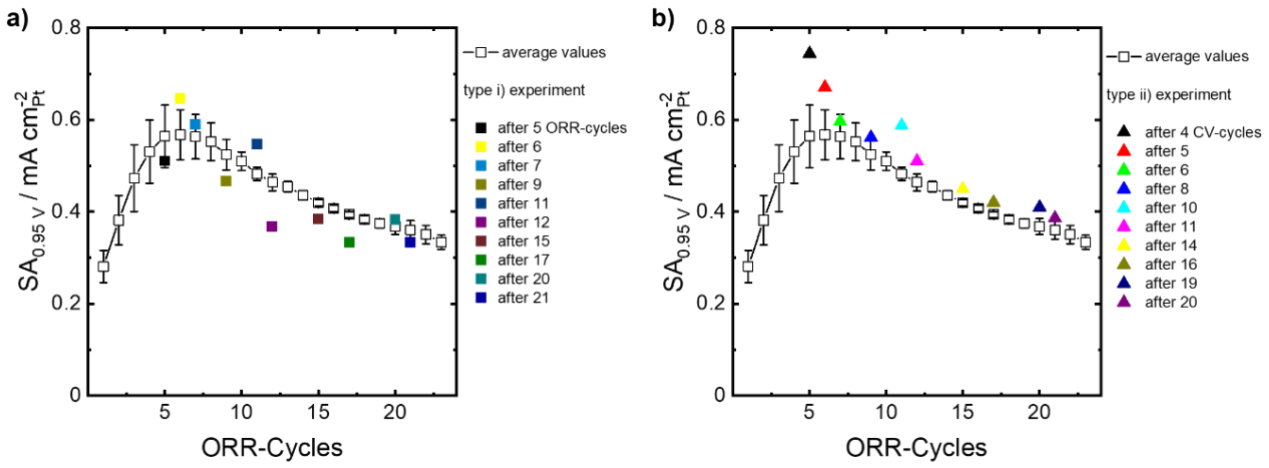

Figure S4: Average values (unfilled squares) for activity progress of PtNiMo/C in O_2 from **Figure 3c**. Additionally specific activity data points a) after ORR-cycles (filled squares, type i) and b) after CV-cycles (filled triangles, type ii). Potential range: 0.05-1.20 V_{RHE} at 20 mV s^{-1}, ORR with rotation at 1600 rpm in O_2 saturated 0.1 M $HClO_4$ solution.

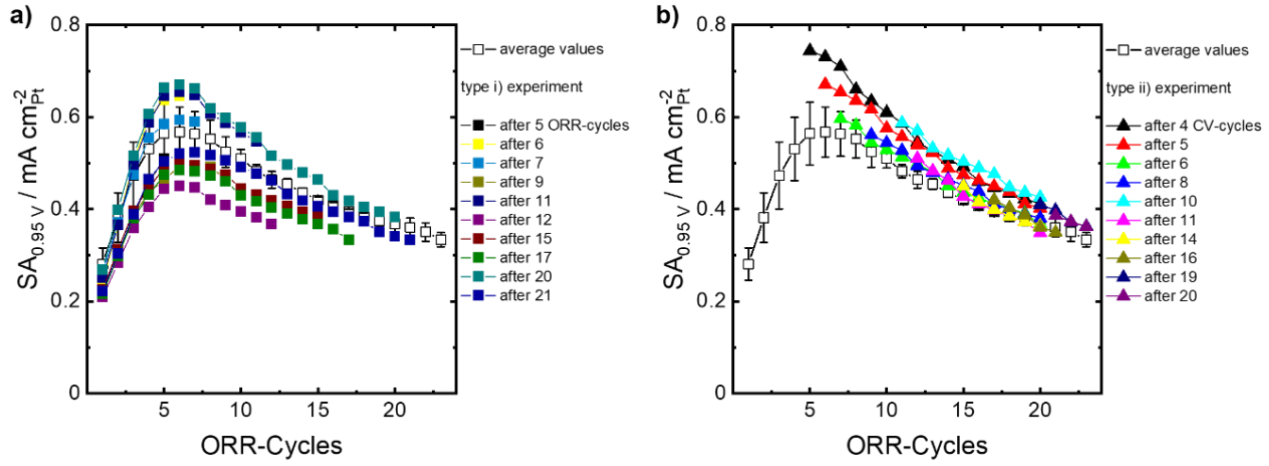

Figure S5: Activity development of each selected cycle number a) up to the point in O_2 (filled squares) and b) after cycling in N_2 (filled triangles), respectively. Repeating SA screening with different catalyst inks (unfilled squares) for PtNiMo/C. Potential range: 0.05-1.20 V_{RHE} at 20 mV s^{-1}, ORR recorded at 1600 rpm rotation in saturated 0.1 M $HClO_4$ solution.

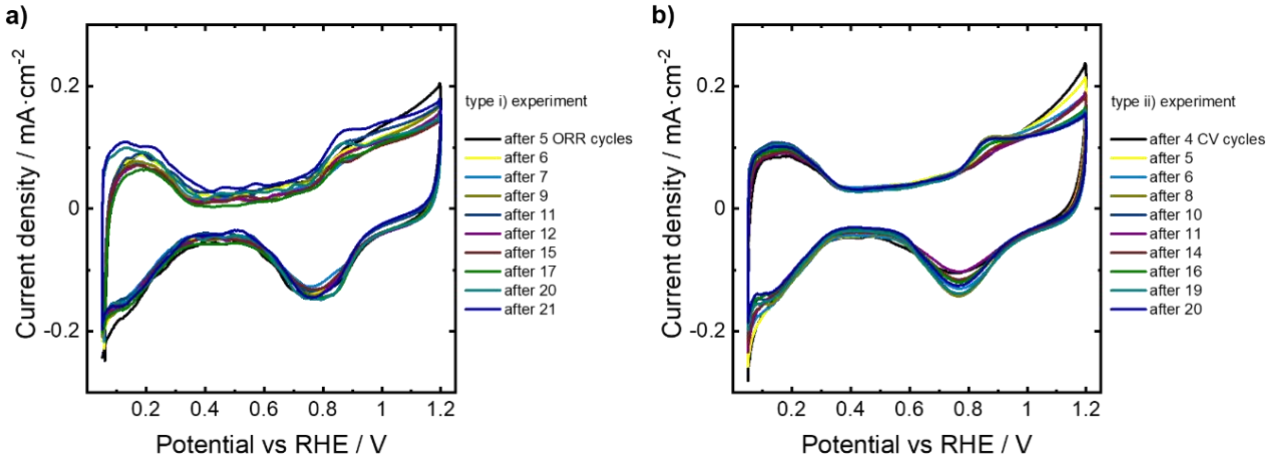

Figure S6: Comparison of CVs after different a) ORR cycles (type i) and b) CV cycles (type ii) in N_2 saturated 0.1 M $HClO_4$ solution. Potential range 0.05-1.20 V_{RHE} and scan rate at 20 mV s^{-1}.

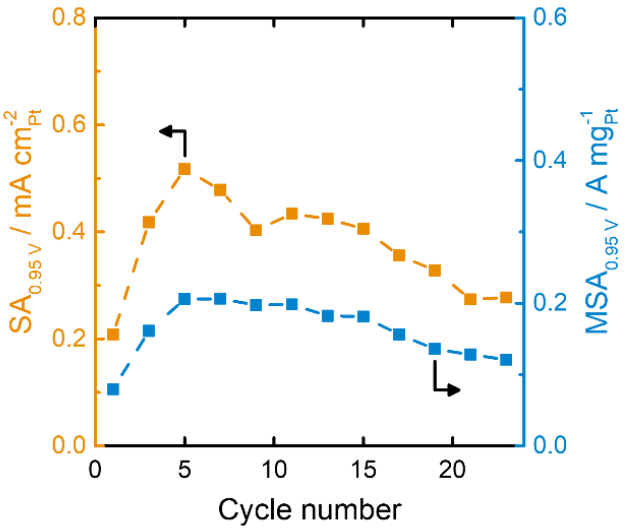

Figure S7: Electrolyte refreshing after each cycle in alternating N_2/O_2 atmosphere at 0.95 V_{RHE}. Potential range: 0.05-1.20 V_{RHE}, SA recorded at 20 mV s^{-1} and 1600 rpm rotation in O_2-saturated 0.1 M $HClO_4$.

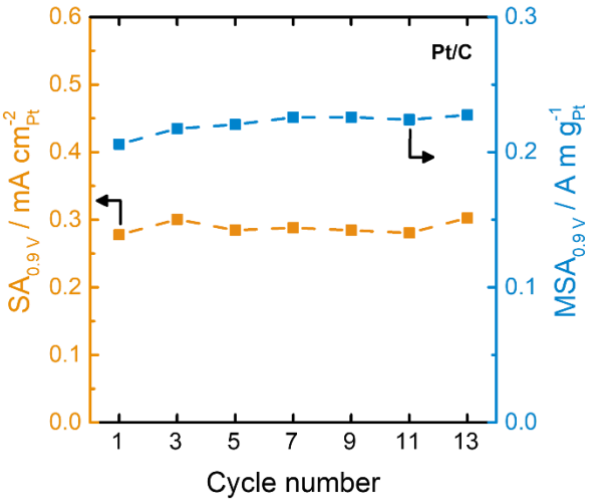

Figure S8: Comparison measurement with Pt/C catalyst. Electrolyte refreshing after each cycle in alternating N_2/O_2 atmosphere at 0.9 V_{RHE}. Potential range: 0.05-1.20 V_{RHE}, SA recorded at 20 mV s^{-1} and 1600 rpm rotation in O_2-saturated 0.1 M $HClO_4$.

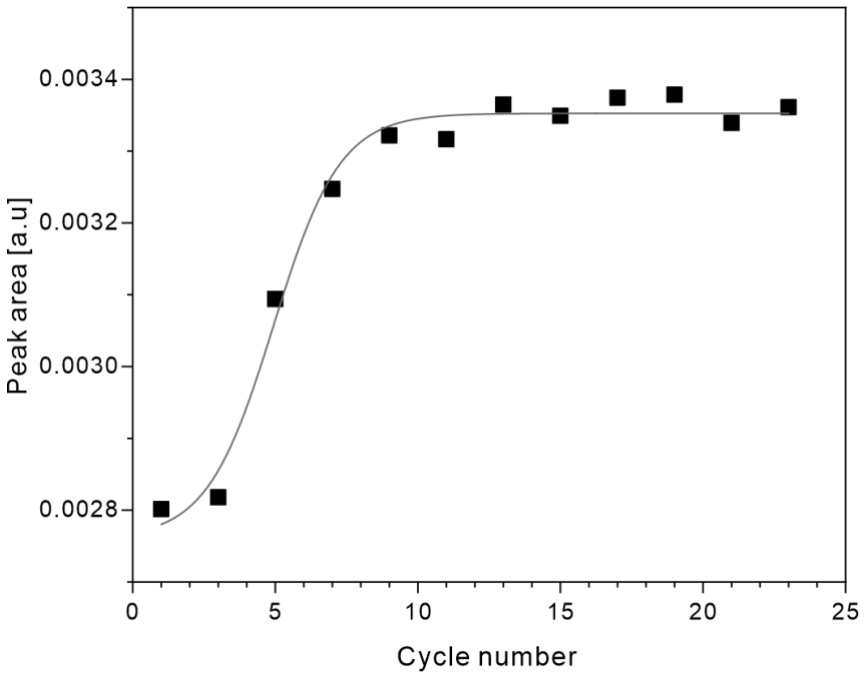

Figure S9: Peak area determined from CO stripping experiment shown in **Figure 8b**.

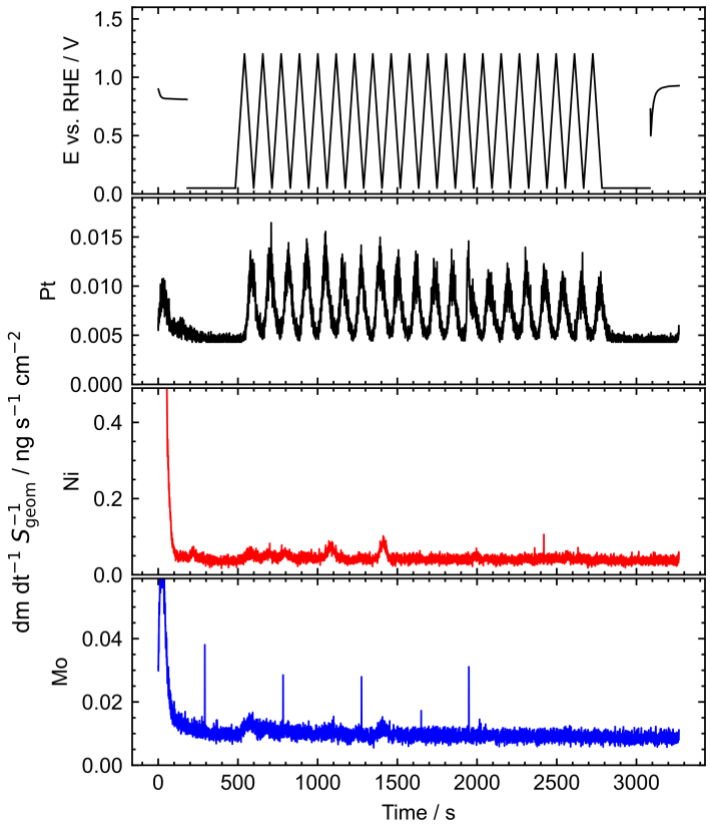

Figure S10: Electrochemical online scanning flow cell ICP-MS measurements in Ar saturated 0.1 M $HClO_4$ electrolyte. 20 CVs between 0.05V_{RHE} and 1.2 V_{RHE} were performed at a cycling rate of 20 mV s^{-1}, before holding 0.05 V_{RHE} for 300 s again.

References

[23] M. George, G.-R. Zhang, N. Schmitt, K. Brunnengräber, D. J. S. Sandbeck, K. J. J. Mayrhofer, S. Cherevko, B. J. M. Etzold, *ACS Catal.* **2019**, *9*, 8682–8692.

[29] X. Huang, Z. Zhao, L. Cao, Y. Chen, E. Zhu, Z. Lin, M. Li, A. Yan, A. Zettl, Y. M. Wang, *Science (1979)* **2015**, *348*, 1230–1234.

[35] M. K. Carpenter, T. E. Moylan, R. S. Kukreja, M. H. Atwan, M. M. Tessema, *J. Am. Chem. Soc.* **2012**, *134*, 8535–8542.

[48] Y. Garsany, O. A. Baturina, K. E. Swider-Lyons, S. S. Kocha, *Anal. Chem.*, **2010**, *82*, 6321-6328.